



# Synthesis and self-assembly of dibenzo[*jk,mn*]naphtho[2,1,8-*fgh*]thebenidinium derivates

Dongqing Wu, Xinliang Feng, Masayoshi Takase, Monika C. Haberecht, Klaus Müllen \*

Max Planck Institute for Polymer Research, Ackermannweg 10, D-55128 Mainz, Germany

## ARTICLE INFO

### Article history:

Received 29 May 2008

Received in revised form 29 July 2008

Accepted 20 August 2008

Available online 27 August 2008

## ABSTRACT

A novel synthetic method toward nitrogen containing positively charged dibenzo[*jk,mn*]naphtho[2,1,8-*fgh*]thebenidinium (DBNT, **1**) salts was developed. In this method, the undehydrogenated precursor of DBNT, 14-phenyl-14-dibenzo[*aj*]acridinium salt (**6**), was produced directly from the reaction between 14-phenyl-14-dibenzo[*aj*]xanthylium (**2**) and amine/aniline in reasonable yield. Various DBNT salts with different alkyl and alkylphenyl chains were synthesized in this two-step method. The self-assembly behavior of two alkylated DBNT salts, **1c** and **1f**, was studied in this work. Due to the different substituents and counterions, compound **1c** formed nanoscale wirelike fibers, and helical aggregates were obtained from **1f**, in their methanolic solutions.

© 2008 Elsevier Ltd. All rights reserved.

## 1. Introduction

In recent years, polycyclic aromatic hydrocarbons (PAHs) have attracted great attention from physicists, chemists, and material scientists due to the excellent electronic and optoelectronic properties, unique supramolecular behavior, and promising applications in organic electronics.<sup>1–3</sup> The incorporation of neutral nitrogen atoms into the aromatic framework of PAHs, which can not only influence their physical and chemical properties but also modify their supramolecular behavior, is one of the most widely used methods to obtain novel organic materials based on PAHs.<sup>4–11</sup> However, research work on nitrogen containing positively charged PAHs is still rare, mainly because of the synthetic difficulties.<sup>12–14</sup> Dibenzo[*jk,mn*]naphtho[2,1,8-*fgh*]thebenidinium (DBNT, **1**, Chart 1) salts are so far the largest nitrogen containing positively charged PAHs (including 27 conjugated carbon atoms). The reported synthetic route toward the phenyl-substituted derivative, 14-phenyl-DBNT hexafluorophosphate (**1a**), required multisteps with a total yield of less than 5% (Scheme 1).<sup>14</sup> Therefore, the development of a versatile and efficient synthetic strategy toward different DBNT derivates is urgently required in order to investigate their chemical/physical properties and potential applications.

Herein, we present a novel synthetic pathway to DBNT salts starting from 14-phenyl-14-dibenzo[*aj*]xanthylium salts (**2**) as the key building blocks. In this method, various DBNT derivates with different alkyl or alkylphenyl substituents on their nitrogen atoms (the 14-position of DBNT) were synthesized in two steps. The

DBNT derivatives were composed of hydrophilic aromatic core and hydrophobic substituents (alkyl/alkylphenyl chains) as amphiphilic aromatic molecules. One-dimensional (1D) nanofibers were obtained from these molecules simply by drop-casting their methanolic solutions on silicon wafer, and the morphology of the nanofibers exhibited obvious dependence on the alkyl chain length and counterions of DBNTs.

## 2. Results and discussion

Compound **1a**, which is the only DBNT salt reported so far, was synthesized by A.C. Benniston and his co-workers very recently (Scheme 1a).<sup>14</sup> Adapted from the work previously reported by W. Dilthey et al.,<sup>15,16</sup> their synthetic procedure started with the condensation of *N*-phenyl-2-naphthylamine, benzaldehyde, and 2-naphthol to produce 7,14-diphenyl-7,14-dihydrodibenzo[*aj*]acridine (**4**). The oxidation of **4** with MnO<sub>2</sub> in the dark resulted in 7,14-diphenyl-7,14-dihydrodibenzo[*aj*]acridin-14-ol (**5**). Dehydration of **5** by HCl and subsequent ion exchange with potassium hexafluorophosphate (KPF<sub>6</sub>) gave 7-phenyl-14-phenyl-dibenzo[*aj*]acridinium hexafluorophosphate (**6b**). Final irradiation of the solution of **6b** with sunlight resulted in the dehydrogenated product **1a**.

This synthetic route was obviously inefficient. First, the oxidation of **5** had to be operated strictly in the dark because any exposure to light caused a drastic decrease in the yield.<sup>14</sup> On the other hand, since the substituted phenyl group on the nitrogen atom of **1a** was rigorously defined in the first step, it meant that any attempt to change the substituted group had to start from different 2-naphthylamines at the beginning, where the synthesis was both tedious and uneconomical. Accordingly, an alternative synthetic

\* Corresponding author. Fax: +49 6131 379 350.

E-mail address: [muellen@mpip-mainz.mpg.de](mailto:muellen@mpip-mainz.mpg.de) (K. Müllen).

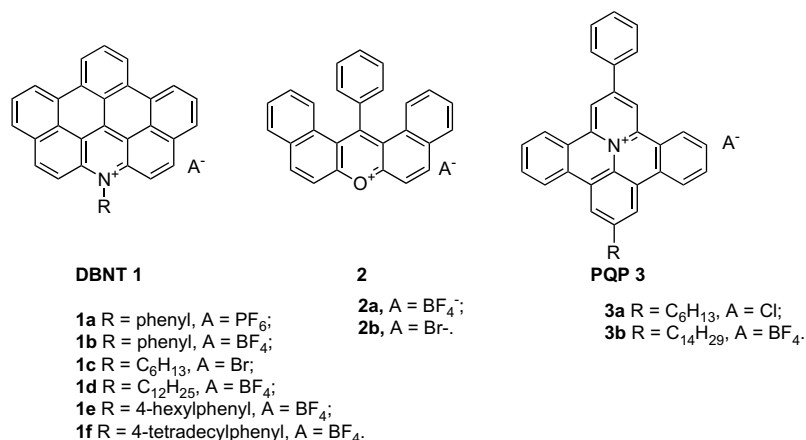
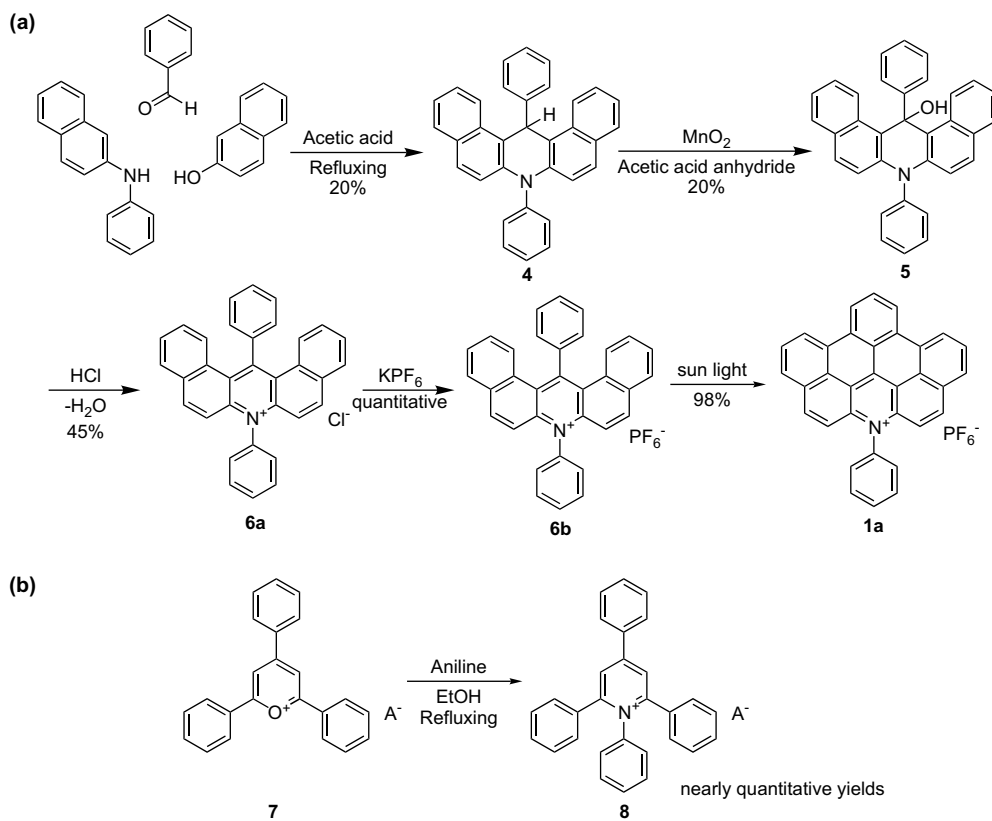


**Chart 1.** Dibenzo[*jk,mn*]naphtho[2,1,8-*fgh*]thebenidinium (DBNT, **1**), 14-phenyl-14-dibenzo[*aj*]xanthylium salts (**2**), and 2-phenyl-benzo[8,9]quinolizino[4,5,6,7-*fed*]-phenanthridinium (PQP, **3**) salts.

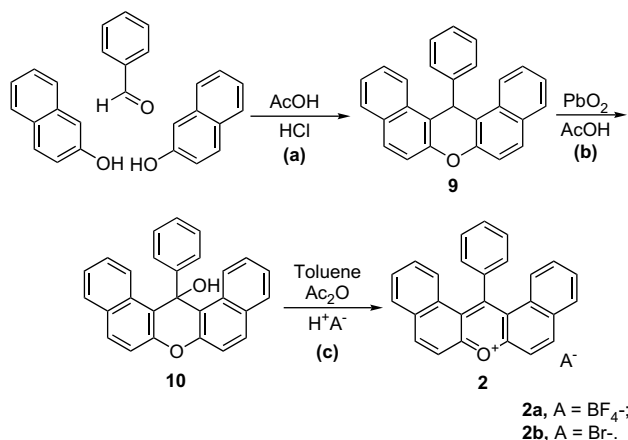


**Scheme 1.** (a) Banniston's method to 14-phenyl-dibenzo[*jk,mn*]naphtho[2,1,8-*fgh*]thebenidinium hexafluorophosphate (PDBNTPF<sub>6</sub>, **1a**); (b) the synthetic pathway to PQP salts.

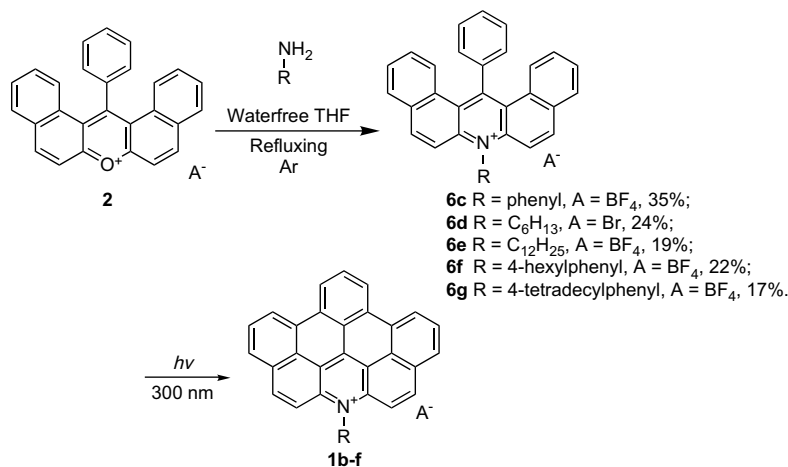
method was required to avoid these disadvantages and simplify the synthetic protocols. In our previous study on the synthesis of 2-phenyl-benzo[8,9]quinolizino[4,5,6,7-*fed*]phenanthridinium (PQP, **3**) salts, various nitrogen containing 1,2,4,6-tetraphenylpyridinium (**8**), which are the precursors of PQP salts, were obtained in nearly quantitative yields by the simple reaction between oxygen containing 2,4,6-triphenylpyrylium (**7**) and anilines (Scheme 1b).<sup>13,17</sup> Therefore, in our opinion, compound **2** could be viewed as the derivative of **7** with extended aromatic core. The same reaction between **7** and aniline could be expected for **2** and thus undehydrogenated precursors **6** could be produced in a novel approach. This meant that the synthesis of DBNT salts **1** could be greatly simplified.

The most important building block in our method, compound **2** was synthesized by following a literature procedure (Scheme 2): Claisen condensation between 2 equiv of 2-naphthol and 1 equiv of benzaldehyde with concentrated hydrochloric acid as the catalyst in glacial acetic acid resulted in 14-phenyl-14H-dibenzo[*aj*]xanthenone (**9**) in 60% yield.<sup>18</sup> Compound **9** was then oxidized to 14-phenyl-14-hydroxy-dibenzo[*aj*]xanthenone (**10**) by PbO<sub>2</sub> in acetic acid at 100 °C (yield 95%). Subsequent treatment of **10** with inorganic acids (H<sup>+</sup>A<sup>-</sup> such as HBF<sub>4</sub> and HBr) in acetic acid anhydride and toluene at 0 °C produced **2** as red powder in nearly quantitative yields.<sup>19</sup>

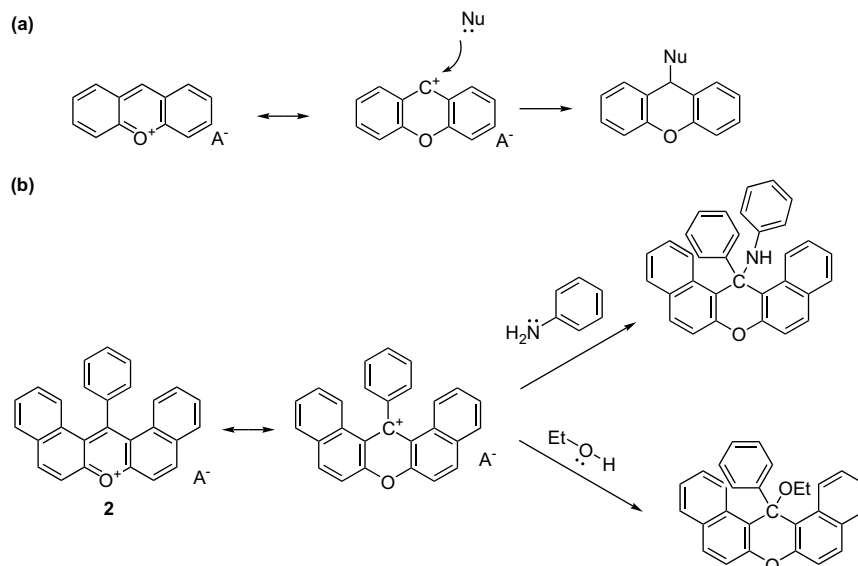
In our work (Scheme 3), the reaction between **2** and aniline/amine in anhydrous THF under argon atmosphere did give



**Scheme 2.** Synthetic pathway toward 14-phenyl-14-dibenzo[*a,j*]xanthenylium salts (**2**). (a) Concentrated hydrochloric acid (catalyst), glacial acetic acid, 100 °C, 6 h, yield=60%; (b) PbO<sub>2</sub>, acetic acid, 100 °C, 2 h, yield=95%; (c) inorganic acids in aqueous solution, acetic acid anhydride and toluene (1:1), 0 °C, ca. 30 min, quantitative yields.



**Scheme 3.** Novel synthetic pathway toward DBNT salt **1**. (a) Aniline/amine (1 equiv), anhydrous THF, argon bubbling, refluxing, ca. 6 h; (b) ethanol, rt, *hν*, ca. 24 h, yield=80% (**1b**), 69% (**1c**), 48% (**1d**), 67% (**1e**), and 43% (**1f**).



**Scheme 4.** (a) The literature reported reaction between xanthenylium derivatives and nucleophilic reagents; (b) the side reaction of **2** and aniline and ethanol.

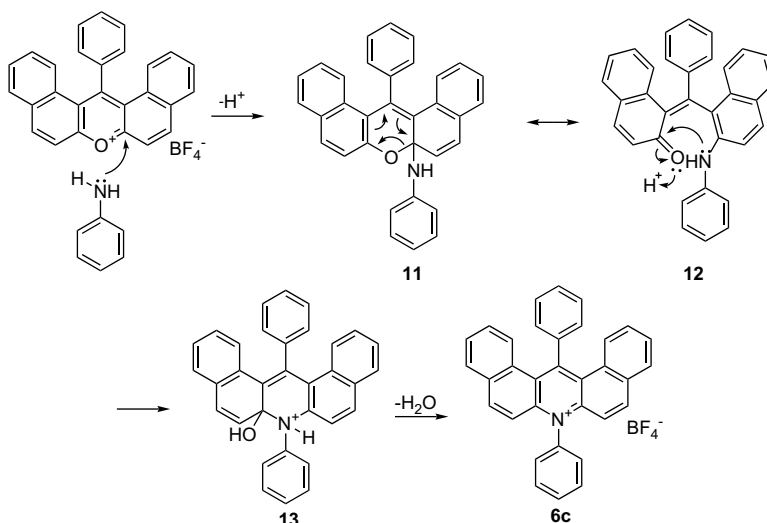
compound **6** in moderate yields. As far as we know, the similar conversion of xanthenylium to corresponding acridinium has so far never been reported. In general, the reactions between xanthenylium salts and nucleophilic reagents mainly led to the addition reactions on their C-9 position (the carbon atom on the *para* position of oxygen atom, Scheme 4a).<sup>20–22</sup> The experimental results were consistent with molecular-orbital calculations of xanthenylium derivatives.<sup>23,24</sup> In the case of **2**, such addition products of aniline in reaction mixture could also be detected by FD MS spectrometry (not shown). It was believed that the steric hindrance on the 14-position of **2** reduced the amount of addition products and enabled us to obtain **6** in reasonable yields.

Another side reaction, the addition between compound **2** and protic solvents such as water, methanol, and ethanol could also decrease the yield of **6** (Scheme 4b). Initially, ethanol was selected as the solvent because it was the most common solvent for the preparation of pyridinium salts or pyrylium salts.<sup>13,17</sup> FD MS and <sup>1</sup>H NMR spectra of the resulting reaction mixture (Fig. S1) indicated that the main reaction was the addition of **2** with ethanol. In this work, anhydrous tetrahydrofuran (THF) was chosen as the suitable solvent to avoid this side reaction.

A mechanism for the formation of dibenzo[*a,j*]acridinium **6** from dibenzo[*a,j*]xanthenylium **2** is proposed herein. As shown in Scheme 5, the reaction might experience a nucleophilic C-2 opening/recyclization.<sup>25</sup> During that process, the first C-2 addition between **2** and aniline led to the ring-opening product **12**. Subsequent intramolecular aldol condensation of **12** produced intermediate **13**, and the further dehydration reaction of the latter compound resulted in the recycled product **6**.

As shown in Scheme 3, the final photocyclization of precursors **6** in ethanol under 300 nm UV light and further recrystallization of

(Fig. 1a) was dominated by a strong band located at 305 nm ( $\log \epsilon=4.88$ ) followed by two weak absorption bands at longer wavelength region (348 nm,  $\log \epsilon=4.43$  and 430 nm,  $\log \epsilon=4.00$ ). Compared with **3b**, compound **1f** showed similar absorption bands in which the first main band was at 328 nm ( $\log \epsilon=4.79$ ), and the other two low energy bands were located at 416 ( $\log \epsilon=4.34$ ), and 507 nm ( $\log \epsilon=4.63$ ), respectively. On the other hand, both molecules exhibited structureless emission peaks in their fluorescence spectra. Remarkably, the emission maximum at 535 nm for **1f** was red-shifted by 69 nm compared with **3b** (466 nm). The obvious



Scheme 5. One possible synthetic mechanism of dibenzo[*a,j*]acridinium **6c**.

the precipitates produced the corresponding DBNT salts **1** with various alkyl and alkylphenyl chains. All molecules were characterized by <sup>1</sup>H and <sup>13</sup>C NMR spectroscopies, MALDI-TOF mass spectrometry as well as elemental analysis (Section 4).

## 2.1. UV-vis absorption and fluorescence spectra of DBNT salts

In the interest of understanding the effect of shape and size of the aromatic core on the physical properties of nitrogen containing positively charged PAHs, the UV-vis absorption and fluorescence spectra of PQP **3b** and DBNT **1f** in methanol were recorded and compared in Figure 1. The absorption spectrum of compound **3b**

difference of the absorbance and fluorescence spectra indicated a strong influence of the extension of the size of aromatic core on their photophysical properties, which was similar to other extended PAHs.<sup>26,27</sup>

## 2.2. Self-assembly of DBNT salts

Recently, we investigated the self-assembly behavior of alkylated PQP derivatives in solution and obtained nanoscale aggregates with different morphologies such as fibers and tubes by using PQP salts with different alkyl chains and counterions.<sup>17</sup> In order to obtain a better understanding of the relationship between the

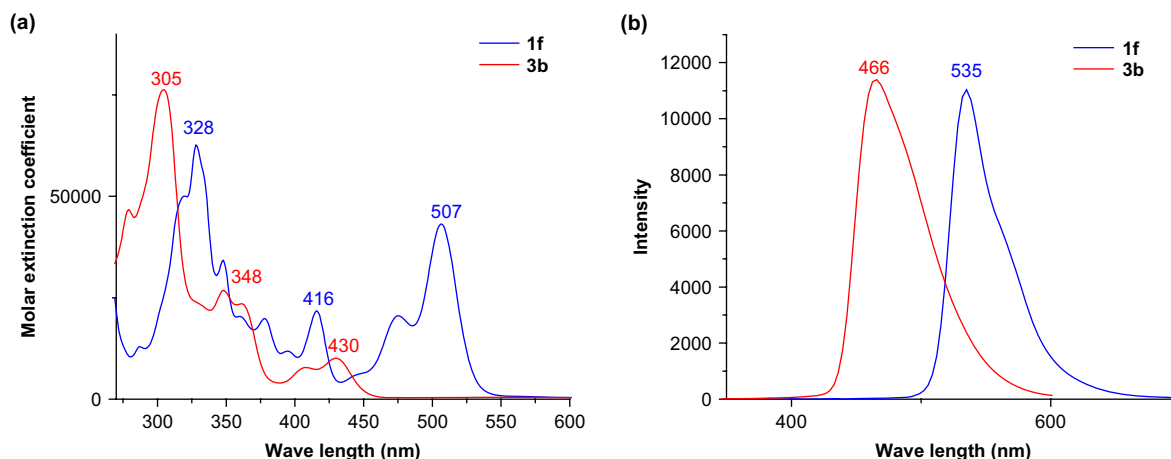


Figure 1. The UV-vis absorption (a) and fluorescence (b) spectra of the different nitrogen containing positively charged PAHs: **3b** (red) and **1f** (blue).

aggregation of nitrogen containing positively charged PAHs and the size of their aromatic cores, the self-assembly behavior of DBNT salts **1c** and **1f** in solution was studied in a similar manner.

The morphology of the aggregates from these two DBNT salts was first investigated by scanning electron microscopy (SEM) after drop-casting their methanolic solutions on silicon wafers. As shown in Figure 2a and b, compound **1c** formed fibrous aggregates and the diameters of these wirelike fibers ranged from 150 to 200 nm, which was similar to the aggregates of PQP salt with hexyl chain and chloride as anion (compound **3a**). In the case of compound **1f** with longer alkyl chain and larger anion, aggregates with fibrous structures were also obtained. It was interesting to note that their diameters were about 50 nm and they contained helical structures (Fig. 2c and d). Such helical structures were also observed for PQP salt with tetradecyl chain and tetrafluoroborate as anion (compound **3b**).<sup>17</sup>

The different morphology of aggregates from the two compounds implied that DBNT salts with different alkyl/alkylphenyl chains might adopt different packing models, which was similar to previous descriptions for PQP salts with different alkyl chains. Subsequent wide angle X-ray scattering (WAXS) measurements of the dry powder of **1c** and **1f** from their methanolic solution confirmed this hypothesis. As shown in Figure 3, the characteristic reflections of lamellar stacking ( $d$  spacings=40.1, 19.6, and 13.2 Å) appeared in the WAXS patterns of compound **1f**, whereas such diffraction peaks could not be observed in the patterns of **1c**.

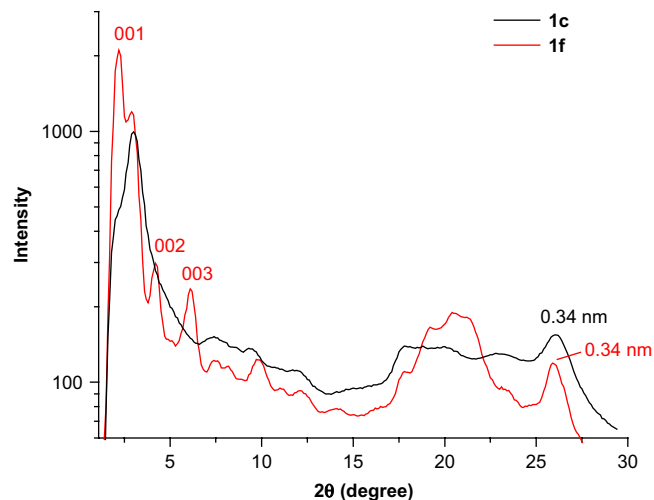


Figure 3. WAXS patterns of the dried powder of **1c** and **1f** obtained from their methanolic solutions.

Therefore, the morphology change of the aggregates formed by **1c** and **1f** could be explained by the packing parameter theory brought forward by Israelachvili.<sup>28–32</sup> This theory proposed that the morphology formed by an amphiphilic molecule was dependent upon its packing parameter,  $P=v/(a_0l_c)$ , where  $v$  was the volume of the

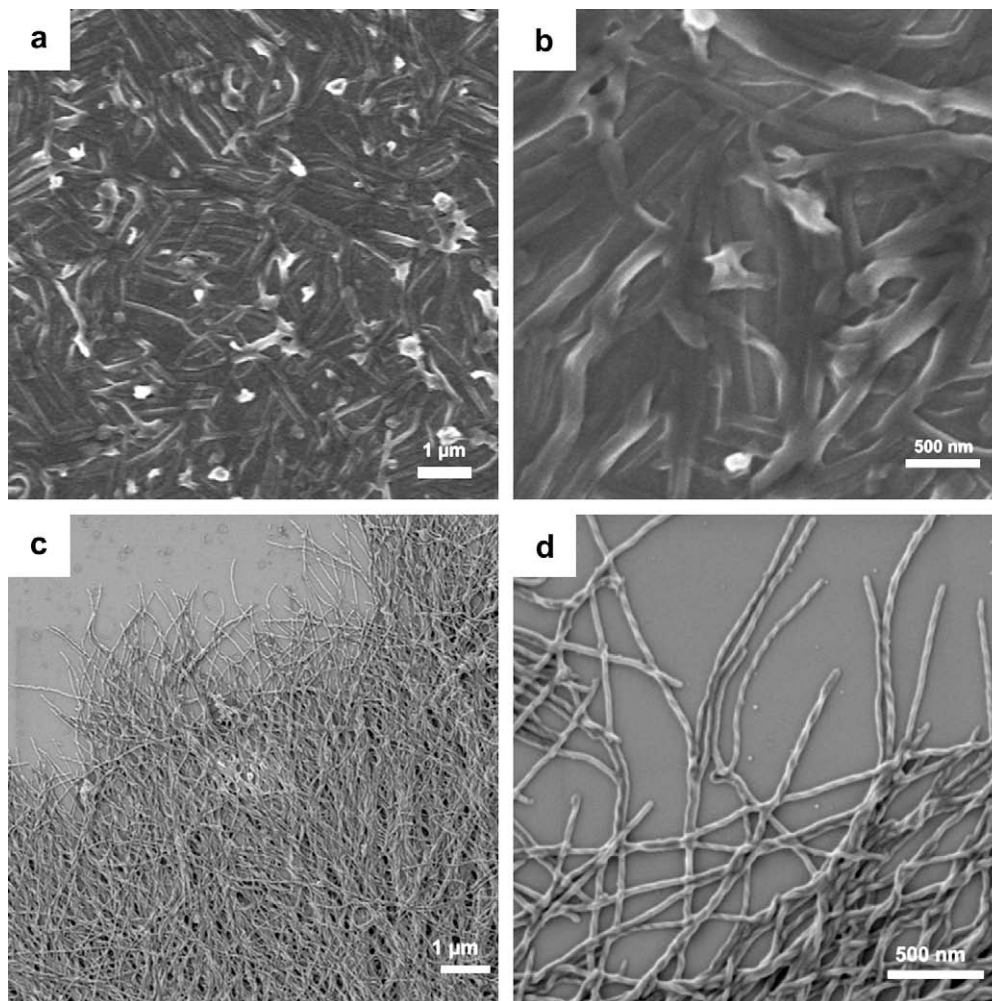


Figure 2. (a) and (b) SEM image of the aggregates formed by **1c**; and (c) and (d) SEM image of the aggregates formed by **1f** ( $1 \times 10^{-3}$  mol/L in methanol, drop-cast on a silicon wafer).

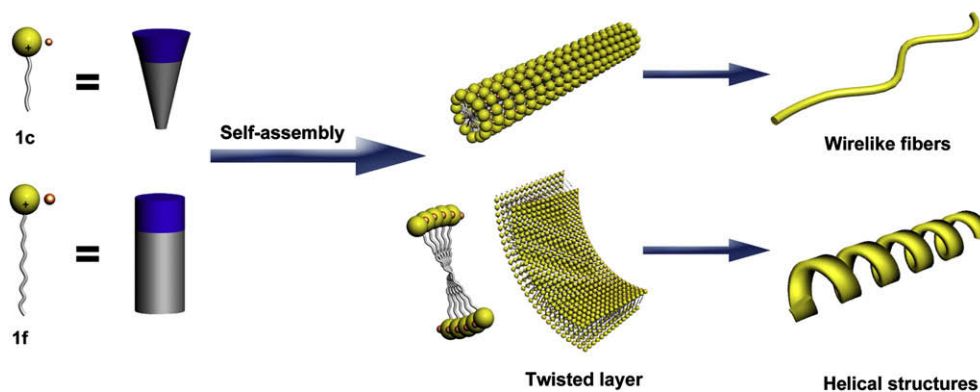


Figure 4. The schematic representation of the self-assembly of **1c** and **1f**.

hydrophobic chain,  $a_0$  was the surface area of the hydrophobic core of the aggregate expressed per molecule in the aggregate (hereafter referred to as the area per molecule), and  $l_c$  was the chain length. If  $P < 1/3$ , spherical and ellipsoidal aggregates were favored morphologies; if  $1/3 < P < 1/2$ , the amphiphile tended to form cylindrical rods; if  $1/2 < P \leq 1$ , bilayer structures such as vesicles, tubes and lamellae were preferred. In the case of these two DBNT salts, the wirelike fibers of **1c** indicated that the packing parameter  $P$  of **1c** was between  $1/3$  and  $1/2$ . With the increase of alkyl chain length, the change of intramolecular interactions such as solvophobic effects caused lower interaction free energies and a smaller optimal surface area per molecule  $a_0$ . As a result, the packing parameter  $P$  of **1f** increased with respect to **1c** and the lamellar aggregates formed accordingly (Fig. 4).<sup>17,33</sup>

On the other hand, the helically coiled shapes of the fibers from **1f** might be caused by the tetrafluoroborate anion as PQP salt **3b**. Such a large anion might disrupt the face-to-face alignment of adjacent molecules, causing them to adopt a slipped orientation. Consequently, neighboring pairs of **1f** were rotated with respect to one another along the axis of the aggregate and a helical aggregate resulted (Fig. 4).<sup>17,34</sup>

Obviously, the similarity in the morphology of aggregates from PQP and DBNT salts indicated that both kinds of nitrogen containing positively charged PAHs had similar self-assembly behavior despite the different size of their aromatic cores. Combining this with the self-assembly behavior of PQP, it was assumed that the governing effects on the morphology of the aggregates from the nitrogen containing positively charged PAHs were the length of their alkyl chains and the size of their counterions.<sup>17,33–35</sup>

### 3. Conclusion

In summary, we have developed a novel synthetic approach toward nitrogen containing DBNT salts. In this method, the underhydrogenated precursors, dibenzo[*a,j*]acridinium salts **6**, were produced directly from the reaction between dibenzo[*a,j*]xanthenylium derivatives **2** and amine/aniline in reasonable yields. Therefore, various DBNT salts with different substituents were successfully synthesized in this two-step method. By drop-casting their methanolic solutions on silicon wafers, two DBNT salts, **1c** and **1f**, with different alkyl and alkylphenyl chains formed one-dimension nanoscaled fibers with relatively different morphologies. The former compound with a hexyl chain aggregated into wirelike fibers, whereas the self-assembly of the latter with a tetradecylphenyl chain produced helical aggregates. The difference in their morphology is due to their different hydrophobic substituents and counterions. These ordered aggregates are expected to be useful as ionic conducting materials<sup>36,37</sup> and the study of their electronic properties is underway in our lab now.

## 4. Experiment part

### 4.1. General information

All starting materials were obtained from commercial suppliers such as Aldrich, Acros, and Fluka and used as received unless otherwise specified. Irradiations with an external UV source were performed with a Rayonet reactor (RPR-200) with 3000 Å lamps in quartz flasks. <sup>1</sup>H and <sup>13</sup>C NMR spectra were recorded on Bruker DPX 250 spectrometer with use of the solvent proton or carbon signal as an internal standard. FD mass spectra were obtained on a VG Instruments ZAB 2-SE-FPD spectrometer. MALDI-TOF mass spectra were measured using a Bruker Reflex II-TOF spectrometer using a 337 nm nitrogen laser and 7,7,8,8-tetracyanoquinodimethane (TCNQ) as matrix. A double graphite monochromator for the Cu K $\alpha$  radiation ( $\lambda=0.154$  nm) was used for the WAXS experiments. SEM measurements were performed on a LEO 1530 field emission scanning electron microscope. The elemental analysis was measured in Institut für Organische Chemie der Johannes Gutenberg-Universität Mainz for: C, N, H: Foss Heraeus vario EL. UV-vis spectra were recorded at room temperature on a Perkin-Elmer Lambda 9 spectrophotometer. Fluorescence spectra were recorded on a SPEX-Fluorolog II (212) spectrometer.

### 4.2. Synthesis

#### 4.2.1. 14-Phenyl-14H-dibenzo[*a,j*]xanthene (**9**)

To a solution of benzaldehyde (50 mmol) and 2-naphthol (100 mmol) in glacial acetic acid (40 mL), concentrated HCl (1 mL) was added dropwise. The solution was heated with oil bath to 100 °C and kept at this temperature until crystallization took place. When the solution was cooled to room temperature, the precipitated product was filtered with suction and recrystallized from glacial acetic acid to give the target compound **9**.

White needles (yield=60%), <sup>1</sup>H NMR (250 MHz, CD<sub>2</sub>Cl<sub>2</sub>, 25 °C):  $\delta$  (ppm)=8.33–8.29 (d, 2H, <sup>3</sup>J(H,H)=10.0 Hz, aromatic), 7.77–7.71 (t, 4H, <sup>3</sup>J(H,H)=7.5 Hz, aromatic), 7.53–7.30 (m, 8H, aromatic), 7.10–7.04 (t, 2H, <sup>3</sup>J(H,H)=7.5 Hz, aromatic), 6.95–6.89 (t, 1H, <sup>3</sup>J(H,H)=7.5 Hz, aromatic), 6.42 (s, 1H, CH); <sup>13</sup>C NMR (62.5 MHz, CD<sub>2</sub>Cl<sub>2</sub>, 25 °C):  $\delta$  (ppm)=148.40, 145.04, 131.10, 130.89, 128.73, 128.62, 128.28, 128.03, 126.63, 126.28, 124.14, 122.43, 117.77, 116.96, 37.83.

FD MS (MW=358.44):  $m/z$ : 358.67.

Elemental analysis: calcd C 90.47%, H 5.06%, O 4.66%; found: C 90.35%, H 5.12%.

#### 4.2.2. 14-Phenyl-14H-dibenzo[*a,j*]xanthen-14-ol (**10**)

Compound **9** (5.6 mmol) and lead dioxide (PbO<sub>2</sub>, 2 g; 8.4 mmol) in glacial acetic acid (50 mL) were stirred while heating on an oil bath at 120 °C for 3 h. The cooled mixture was poured onto crushed

ice and the solid residue was recrystallized from aqueous acetone to give **10**.

White powder (yield=95%),  $^1\text{H}$  NMR (250 MHz,  $\text{CD}_2\text{Cl}_2$ , 25 °C):  $\delta$  (ppm)=8.95–8.91 (d, 2H,  $^3J(\text{H,H})=10.0$  Hz, aromatic), 7.76–7.72 (d, 2H,  $^3J(\text{H,H})=10.0$  Hz, aromatic), 7.69–7.62 (m, 4H, aromatic), 7.35–7.31 (d, 2H,  $^3J(\text{H,H})=10.0$  Hz, aromatic), 7.29–7.22 (m, 4H, aromatic), 7.11–7.05 (t, 2H,  $^3J(\text{H,H})=7.5$  Hz, aromatic), 6.93–6.87 (t, 1H,  $^3J(\text{H,H})=7.5$  Hz, aromatic), 3.12 (s, 1H, OH);  $^{13}\text{C}$  NMR (62.5 MHz,  $\text{CD}_2\text{Cl}_2$ , 25 °C):  $\delta$  (ppm)=132.57, 131.80, 131.70, 129.89, 129.49, 128.17, 127.94, 127.73, 127.53, 127.41, 126.94, 126.86, 125.93, 124.89, 124.81, 118.31.

MALDI-TOF-MS (MW=374.13):  $m/z$ : 374.21.

#### 4.2.3. Dehydration of xanthen-ol (synthesis of **2a** and **2b**)

Compound **10** (5 mmol) in acetic anhydride (15 mL) and toluene (5 mL) were cooled and treated with inorganic acid (ca. 25 mmol) until no further precipitation occurred. The cooled solution was filtered and washed with anhydrous ether to yield **2** as product.

**4.2.3.1. 14-Phenyl-14-dibenzo[a,j]xanthenylium tetrafluoroborate (2a).** Dark red crystals with a golden glimmer (yield=92%),  $^1\text{H}$  NMR (250 MHz,  $\text{CD}_2\text{Cl}_2$ , 25 °C):  $\delta$  (ppm)=8.78–8.74 (d, 2H,  $^{\text{pre}}J(\text{H,H})=10.0$  Hz, aromatic), 8.25–8.21 (d, 2H,  $^3J(\text{H,H})=10.0$  Hz, aromatic), 8.16–8.12 (d, 2H,  $^3J(\text{H,H})=10.0$  Hz, aromatic), 7.91–7.81 (m, 3H, aromatic), 7.75–7.69 (t, 2H,  $^3J(\text{H,H})=7.5$  Hz, aromatic), 7.48–7.36 (m, 4H, aromatic), 7.17–7.14 (d, 2H,  $^3J(\text{H,H})=7.5$  Hz, aromatic);  $^{13}\text{C}$  NMR (62.5 MHz,  $\text{CD}_2\text{Cl}_2$ , 25 °C):  $\delta$  (ppm)=167.30, 159.95, 147.70, 138.67, 133.20, 132.73, 132.40, 132.10, 130.90, 130.08, 129.43, 128.60, 126.73, 122.56, 117.72.

MALDI-TOF-MS (MW=357.13 without anion):  $m/z$ : 357.20.

**4.2.3.2. 14-Phenyl-14-dibenzo[a,j]xanthenylium bromide (2b).** Dark red crystals with a golden glimmer (yield=95%),  $^1\text{H}$  NMR (250 MHz,  $\text{CD}_2\text{Cl}_2$ , 25 °C):  $\delta$  (ppm)=8.75–8.71 (d, 2H,  $^3J(\text{H,H})=10.0$  Hz, aromatic), 8.21–8.17 (d, 2H,  $^3J(\text{H,H})=10.0$  Hz, aromatic), 8.13–8.10 (d, 2H,  $^3J(\text{H,H})=7.5$  Hz, aromatic), 7.90–7.82 (m, 3H, aromatic), 7.74–7.68 (t, 2H,  $^3J(\text{H,H})=7.5$  Hz, aromatic), 7.46–7.35 (m, 4H, aromatic), 7.16–7.12 (d, 2H,  $^3J(\text{H,H})=10.0$  Hz, aromatic);  $^{13}\text{C}$  NMR (62.5 MHz,  $\text{CD}_2\text{Cl}_2$ , 25 °C):  $\delta$  (ppm)=167.51, 159.90, 147.64, 138.61, 133.15, 132.73, 132.40, 132.06, 130.91, 130.08, 129.41, 128.59, 126.67, 122.55, 117.60.

MALDI-TOF-MS (MW=357.13 without anion):  $m/z$ : 357.18.

#### 4.2.4. 7,14-Diphenyldibenzo[a,j]acridinium derivatives

All the aniline/amine were dried according to handbook procedure before use. Compound **2** (2 mmol) and appropriate aniline/amine (2.2 mmol) were added to 15 mL anhydrous THF. The mixture was refluxed for 5 h till the solution turned transparent. After cooling the solution to room temperature, it was concentrated in vacuo to ca. 3 mL. Then the concentrated solution was poured into 400 mL hexane. After filtration, the solid was recrystallized from 20 mL hexane to give the target compound **6**.

**4.2.4.1. 7,14-Diphenyldibenzo[a,j]acridinium tetrafluoroborate (6c).** Golden yellow needles (yield=35%),  $^1\text{H}$  NMR (250 MHz,  $\text{CD}_2\text{Cl}_2$ , 25 °C):  $\delta$  (ppm)=8.50–8.46 (d, 2H,  $^3J(\text{H,H})=10.0$  Hz, aromatic), 8.20–8.16 (d, 2H,  $^3J(\text{H,H})=10.0$  Hz, aromatic), 8.05–8.03 (m, 3H, aromatic), 8.00–7.76 (m, 7H, aromatic), 7.67–7.40 (m, 8H, aromatic);  $^{13}\text{C}$  NMR (62.5 MHz,  $\text{CD}_2\text{Cl}_2$ , 25 °C):  $\delta$  (ppm)=143.00, 140.81, 140.29, 138.72, 132.61, 131.93, 131.62, 131.58, 130.95, 130.04, 129.30, 129.23, 129.02, 128.91, 128.25, 127.93, 125.10.

MALDI-TOF-MS (MW=432.17 without anion):  $m/z$ : 432.26.

**4.2.4.2. 7-Hexyl-14-phenyldibenzo[a,j]acridinium bromide (6d).** Golden yellow powder (yield=24%),  $^1\text{H}$  NMR (250 MHz,  $\text{CD}_2\text{Cl}_2$ , 25 °C):  $\delta$  (ppm)=8.41–8.37 (d, 2H,  $^3J(\text{H,H})=10.0$  Hz, aromatic), 8.11–8.07 (d, 2H,  $^3J(\text{H,H})=10.0$  Hz, aromatic), 8.00–7.95 (m, 3H, aromatic), 7.89–7.66 (m, 7H, aromatic), 7.58–7.36 (m, 3H, aromatic), 5.07–5.03 (t, 2H,  $^3J(\text{H,H})=5.0$  Hz,  $\text{CH}_2$ ), 3.11–3.07 (m, 2H,  $\text{CH}_2$ ), 1.47–1.12 (m, 6H,

$\text{CH}_2$ ), 0.81–0.77 (m, 3H,  $\text{CH}_3$ );  $^{13}\text{C}$  NMR (62.5 MHz,  $\text{CD}_2\text{Cl}_2$ , 25 °C):  $\delta$  (ppm)=143.45, 141.20, 140.71, 139.10, 133.06, 132.37, 132.02, 132.98, 131.25, 130.50, 129.71, 129.60, 127.93, 31.52, 29.54, 27.34, 22.77, 14.11.

MALDI-TOF-MS (MW=440.24 without anion):  $m/z$ : 440.30.

**4.2.4.3. 7-Dodecyl-14-phenyldibenzo[a,j]acridinium tetrafluoroborate (6e).** Golden yellow powder (yield=19%),  $^1\text{H}$  NMR (250 MHz,  $\text{CD}_2\text{Cl}_2$ , 25 °C):  $\delta$  (ppm)=8.45–8.41 (d, 2H,  $^3J(\text{H,H})=10.0$  Hz, aromatic), 8.15–8.11 (d, 2H,  $^3J(\text{H,H})=10.0$  Hz, aromatic), 8.07–8.00 (m, 3H, aromatic), 7.94–7.76 (m, 7H, aromatic), 7.62–7.41 (m, 3H, aromatic), 5.09–5.05 (t, 2H,  $^3J(\text{H,H})=5.0$  Hz,  $\text{CH}_2$ ), 3.12–3.08 (m, 2H,  $\text{CH}_2$ ), 1.50–1.11 (m, 18H,  $\text{CH}_2$ ), 0.82–0.78 (m, 3H,  $\text{CH}_3$ );  $^{13}\text{C}$  NMR (62.5 MHz,  $\text{CD}_2\text{Cl}_2$ , 25 °C):  $\delta$  (ppm)=143.25, 141.00, 140.53, 138.97, 132.96, 132.27, 131.89, 132.78, 131.07, 130.32, 129.55, 129.45, 127.73, 32.82, 31.75, 31.23, 30.34, 29.54, 27.34, 25.08, 22.77, 14.11.

MALDI-TOF-MS (MW=524.33 without anion):  $m/z$ : 524.45.

**4.2.4.4. 14-Phenyl-7-(4-hexylphenyl)dibenzo[a,j]acridinium tetrafluoroborate (6f).** Golden yellow powder (yield=22%),  $^1\text{H}$  NMR (250 MHz,  $\text{CD}_2\text{Cl}_2$ , 25 °C):  $\delta$  (ppm)=8.44–8.40 (d, 2H,  $^3J(\text{H,H})=10.0$  Hz, aromatic), 8.13–8.09 (d, 2H,  $^3J(\text{H,H})=10.0$  Hz, aromatic), 7.94–7.92 (m, 3H, aromatic), 7.90–7.62 (m, 7H, aromatic), 7.55–7.30 (m, 7H, aromatic), 2.97–2.91 (t, 2H,  $\text{CH}_2$ ), 1.91–1.78 (m, 2H,  $\text{CH}_2$ ), 1.46–1.31 (m, 6H,  $\text{CH}_2$ ), 0.95–0.98 (m, 3H,  $\text{CH}_3$ );  $^{13}\text{C}$  NMR (62.5 MHz,  $\text{CD}_2\text{Cl}_2$ , 25 °C):  $\delta$  (ppm)=143.05, 140.87, 140.35, 138.80, 132.68, 131.99, 131.68, 131.70, 131.01, 130.10, 129.38, 129.70, 129.12, 128.97, 128.35, 127.97, 125.15, 35.44, 31.87, 31.08, 28.52, 22.94, 14.19.

MALDI-TOF-MS (MW=516.27 without anion):  $m/z$ : 516.35.

**4.2.4.5. 14-Phenyl-7-(4-tetradecylphenyl)dibenzo[a,j]acridinium tetrafluoroborate (6g).** Golden yellow powder (yield=17%),  $^1\text{H}$  NMR (250 MHz,  $\text{CD}_2\text{Cl}_2$ , 25 °C):  $\delta$  (ppm)=8.43–8.39 (d, 2H,  $^3J(\text{H,H})=10.0$  Hz, aromatic), 8.12–8.08 (d, 2H,  $^3J(\text{H,H})=10.0$  Hz, aromatic), 7.93–7.91 (m, 3H, aromatic), 7.89–7.61 (m, 7H, aromatic), 7.54–7.29 (m, 7H, aromatic), 2.96–2.91 (t, 2H,  $\text{CH}_2$ ), 1.91–1.78 (m, 2H,  $\text{CH}_2$ ), 1.46–1.16 (m, 22H,  $\text{CH}_2$ ), 0.88–0.85 (m, 3H,  $\text{CH}_3$ );  $^{13}\text{C}$  NMR (62.5 MHz,  $\text{CD}_2\text{Cl}_2$ , 25 °C):  $\delta$  (ppm)=143.06, 140.85, 140.37, 138.81, 132.66, 131.97, 131.66, 131.68, 130.92, 130.05, 129.32, 129.68, 129.10, 128.95, 128.33, 127.92, 125.10, 36.05, 33.11, 32.11, 30.85, 30.56, 29.62, 23.79, 14.49.

MALDI-TOF-MS (MW=628.39 without anion):  $m/z$ : 628.51.

#### 4.2.5. Photocyclization

1 mmol **6** was dissolved in 200 mL absolute ethanol. The ethanolic solution was irradiated with 300 nm UV lamp. After 72 h, the solid product was filtered off. The resulted solid was recrystallized in ethanol to give the DBNT salts **1**.

**4.2.5.1. 14-Phenyl-dibenzo[jk,mn]naphtho[2,1,8-fgh]thebenidinium tetrafluoroborate (1b).** Golden red needles (yield=85%),  $^1\text{H}$  NMR (250 MHz,  $\text{CD}_2\text{Cl}_2$ , 25 °C):  $\delta$  (ppm)=9.35–9.32 (d, 2H,  $^3J(\text{H,H})=7.5$  Hz, aromatic), 9.18–9.15 (d, 2H,  $^3J(\text{H,H})=7.5$  Hz, aromatic), 8.82–8.78 (d, 2H,  $^3J(\text{H,H})=10.0$  Hz, aromatic), 8.68–8.65 (d, 2H,  $^3J(\text{H,H})=7.5$  Hz, aromatic), 8.40–8.34 (t, 3H,  $^3J(\text{H,H})=7.5$  Hz, aromatic), 8.08–8.06 (t, 3H,  $^3J(\text{H,H})=2.5$  Hz, aromatic), 7.88–7.84 (m, 4H, aromatic);  $^{13}\text{C}$  NMR (62.5 MHz,  $\text{CD}_2\text{Cl}_2$ , 25 °C):  $\delta$  (ppm)=148.50, 140.49, 139.55, 133.92, 133.41, 132.13, 131.65, 130.19, 130.15, 129.89, 128.14, 127.09, 124.18, 122.59, 118.66, 117.17.

MALDI-TOF-MS (MW=428.14 without anion):  $m/z$ : 428.21.

Elemental analysis: calcd C 76.92%, H 3.52%, B 2.10%, F 14.25%, N 2.72%; found: C 76.95%, H 3.72%, N 2.61%.

**4.2.5.2. 14-Hexyl-dibenzo[jk,mn]naphtho[2,1,8-fgh]thebenidinium bromide (1c).** Golden red powder (yield=69%),  $^1\text{H}$  NMR (250 MHz,  $\text{CD}_2\text{Cl}_2$ , 25 °C):  $\delta$  (ppm)=8.49–8.46 (d, 2H,  $^3J(\text{H,H})=7.5$  Hz,

aromatic), 8.27–8.24 (d, 2H,  $^3J(\text{H,H})=7.5$  Hz, aromatic), 8.16–8.09 (m, 4H, aromatic), 7.79–7.73 (m, 6H, aromatic), 7.36–7.32 (m, 1H,  $^3J(\text{H,H})=5.0$  Hz, aromatic), 5.16–5.12 (t, 2H,  $^3J(\text{H,H})=5.0$  Hz,  $\text{CH}_2$ ), 3.15–3.10 (m, 2H,  $\text{CH}_2$ ), 1.50–1.18 (m, 6H,  $\text{CH}_2$ ), 0.83–0.80 (m, 3H,  $\text{CH}_3$ );  $^{13}\text{C}$  NMR (62.5 MHz,  $\text{CD}_2\text{Cl}_2$ , 25 °C):  $\delta$  (ppm)=142.60, 139.89, 138.15, 137.31, 133.78, 131.11, 129.56, 128.55, 126.13, 122.88, 120.99, 116.59, 113.44, 110.75, 104.62, 32.31, 30.03, 29.97, 29.74, 23.07, 14.26.

MALDI-TOF-MS (MW=428.14 without anion):  $m/z$ : 428.21.

Elemental analysis: calcd C 76.74%, H 5.07%, Br 15.47%, N 2.71%; found: C 77.24%, H 4.53%, N 2.49%.

4.2.5.3. 14-Dodecyl-dibenzo[*jk,mn*]naphtho[2,1,8-*fg*h]thebenidinium tetrafluoroborate (**1d**). Golden red powder (yield=48%),  $^1\text{H}$  NMR (250 MHz,  $\text{CD}_2\text{Cl}_2$ , 25 °C):  $\delta$  (ppm)=8.46–8.43 (d, 2H,  $^3J(\text{H,H})=7.5$  Hz, aromatic), 8.24–8.21 (d, 2H,  $^3J(\text{H,H})=7.5$  Hz, aromatic), 8.13–8.04 (m, 4H, aromatic), 7.79–7.73 (m, 6H, aromatic), 7.33–7.29 (m, 1H,  $^3J(\text{H,H})=5.0$  Hz, aromatic), 5.14–5.10 (t, 2H,  $^3J(\text{H,H})=5.0$  Hz,  $\text{CH}_2$ ), 2.04–2.02 (m, 2H,  $\text{CH}_2$ ), 1.76–1.71 (m, 2H,  $\text{CH}_2$ ), 1.48–1.32 (m, 18H,  $\text{CH}_2$ ), 0.81–0.79 (m, 3H,  $\text{CH}_3$ );  $^{13}\text{C}$  NMR (62.5 MHz,  $\text{CD}_2\text{Cl}_2$ , 25 °C):  $\delta$  (ppm)=142.51, 139.80, 138.06, 137.22, 133.70, 131.03, 129.48, 128.45, 126.04, 122.79, 120.91, 116.50, 113.35, 110.66, 104.53, 32.28, 31.36, 30.23, 29.85, 29.64, 29.29, 22.62, 14.31.

MALDI-TOF-MS (MW=520.30 without anion):  $m/z$ : 520.11.

Elemental analysis: calcd C 77.10%, H 6.30%, B 1.78%, F 12.51%, N 2.31%; found: C 77.29%, H 6.11%, N 2.53%.

4.2.5.4. 14-(4-Hexylphenyl)-dibenzo[*jk,mn*]naphtho[2,1,8-*fg*h]thebenidinium tetrafluoroborate (**1e**). Golden red powder (yield=67%),  $^1\text{H}$  NMR (250 MHz,  $\text{CD}_2\text{Cl}_2$ , 25 °C):  $\delta$  (ppm)=9.41–9.38 (d, 2H,  $^3J(\text{H,H})=7.5$  Hz, aromatic), 9.29–9.26 (d, 2H,  $^3J(\text{H,H})=7.5$  Hz, aromatic), 8.74–8.70 (d, 2H,  $^3J(\text{H,H})=10.0$  Hz, aromatic), 8.61–8.59 (d, 2H,  $^3J(\text{H,H})=7.5$  Hz, aromatic), 8.53–8.47 (t, 1H,  $^3J(\text{H,H})=7.5$  Hz, aromatic), 8.42–8.36 (t, 2H,  $^3J(\text{H,H})=7.5$  Hz, aromatic), 7.85–7.74 (m, 4H, aromatic), 7.55–7.52 (d, 2H,  $^3J(\text{H,H})=7.5$  Hz, aromatic); 2.94–2.88 (t, 2H,  $^3J(\text{H,H})=7.5$  Hz,  $\text{CH}_2$ ), 1.84–1.76 (m, 2H,  $\text{CH}_2$ ), 1.46–1.35 (m, 6H,  $\text{CH}_2$ ), 0.94–0.89 (m, 3H,  $\text{CH}_3$ );  $^{13}\text{C}$  NMR (62.5 MHz,  $\text{CD}_2\text{Cl}_2$ , 25 °C):  $\delta$  (ppm)=148.41, 140.40, 139.51, 133.89, 133.36, 132.09, 131.61, 130.15, 130.11, 129.86, 128.09, 127.07, 124.10, 122.53, 118.59, 117.11, 36.27, 32.13, 31.74, 29.48, 23.05, 14.29.

MALDI-TOF-MS (MW=512.24 without anion):  $m/z$ : 512.22.

Elemental analysis: calcd C 78.14%, H 5.04%, B 1.80%, F 12.68%, N 2.34%; found: C 77.94%, H 4.83%, N 2.25%.

4.2.5.5. 14-(4-Tetradecylphenyl)-dibenzo[*jk,mn*]naphtho[2,1,8-*fg*h]thebenidinium tetrafluoroborate (**1f**). Golden red powder (yield=43%),  $^1\text{H}$  NMR (250 MHz,  $\text{CD}_2\text{Cl}_2$ , 25 °C):  $\delta$  (ppm)=9.05–9.01 (d, 2H,  $^3J(\text{H,H})=7.5$  Hz, aromatic), 8.84–8.81 (d, 2H,  $^3J(\text{H,H})=7.5$  Hz, aromatic), 8.69–8.65 (d, 2H,  $^3J(\text{H,H})=10.0$  Hz, aromatic), 8.52–8.49 (d, 2H,  $^3J(\text{H,H})=7.5$  Hz, aromatic), 8.26–8.20 (t, 1H,  $^3J(\text{H,H})=7.5$  Hz, aromatic), 8.17–8.11 (t, 2H,  $^3J(\text{H,H})=7.5$  Hz, aromatic), 7.84–7.78 (m, 4H, aromatic), 7.59–7.55 (d, 2H,  $^3J(\text{H,H})=10.0$  Hz, aromatic), 2.99–2.93 (t, 2H,  $^3J(\text{H,H})=7.5$  Hz,  $\text{CH}_2$ ), 1.91–1.85 (m, 2H,  $\text{CH}_2$ ), 1.54–1.21 (m, 22H,  $\text{CH}_2$ ), 0.85–0.83 (m, 3H,  $\text{CH}_3$ );  $^{13}\text{C}$  NMR (62.5 MHz,  $\text{CD}_2\text{Cl}_2$ , 25 °C):  $\delta$  (ppm)=148.70, 140.69, 139.78, 134.18, 133.55, 132.33, 131.81, 130.40, 130.60, 130.08, 128.33, 127.38, 124.39, 122.81, 118.92, 117.41, 37.11, 33.15, 32.73, 30.92, 30.70, 30.65, 29.88, 22.98, 14.55.

MALDI-TOF-MS (MW=624.36 without anion):  $m/z$ : 624.42.

Elemental analysis: calcd C 79.32%, H 6.51%, B 1.52%, F 10.68%, N 1.97%; found: C 79.72%, H 6.22%, N 1.95%.

## Acknowledgements

This work was financially supported by the Max Planck Society through the program ENERCHEM, the German Science Foundation (Korean–German IRTG), and DFG Priority Program SPP 1355.

## Supplementary data

Supplementary data associated with this article can be found in the online version, at doi:10.1016/j.tet.2008.08.063.

## References and notes

- Grimdale, A. C.; Müllen, K. *Angew. Chem., Int. Ed.* **2005**, *44*, 5592.
- Hoeben, F. J. M.; Jonkheijm, P.; Meijer, E. W.; Schenning, A. *Chem. Rev.* **2005**, *105*, 1491.
- Wu, J. S.; Pisula, W.; Müllen, K. *Chem. Rev.* **2007**, *107*, 718.
- Bolger, J.; Gourdon, A.; Ishow, E.; Launay, J. P. *J. Chem. Soc., Chem. Commun.* **1995**, 1799.
- Bolger, J.; Gourdon, A.; Ishow, E.; Launay, J. P. *Inorg. Chem.* **1996**, *35*, 2937.
- Kumar, S.; Rao, D. S. S.; Prasad, S. K. *J. Mater. Chem.* **1999**, *9*, 2751.
- Pieterse, K.; van Hal, P. A.; Kleppinger, R.; Vekemans, J.; Janssen, R. A. J.; Meijer, E. W. *Chem. Mater.* **2001**, *13*, 2675.
- Lemaire, V.; Da Silva Filho, D. A.; Coropceanu, V.; Lehmann, M.; Geerts, Y.; Piris, J.; Debije, M. G.; Van de Craats, A. M.; Senthilkumar, K.; Siebbeles, L. D. A.; Warman, J. M.; Bredas, J. L.; Cornil, J. *J. Am. Chem. Soc.* **2004**, *126*, 3271.
- Barlow, S.; Zhang, Q.; Kaafarani, B. R.; Risko, C.; Amy, F.; Chan, C. K.; Domercq, B.; Starikova, Z. A.; Antipin, M. Y.; Timofeeva, T. V.; Kippelen, B.; Bredas, J. L.; Kahn, A.; Marder, S. R. *Chem.—Eur. J.* **2007**, *13*, 3537.
- Bosdet, M. J. D.; Piers, W. E.; Sorensen, T. S.; Parvez, M. *Angew. Chem., Int. Ed.* **2007**, *46*, 4940.
- Takase, M.; Enkelmann, V.; Sebastiani, D.; Baumgarten, M.; Müllen, K. *Angew. Chem., Int. Ed.* **2007**, *46*, 5524.
- Katritzky, A. R.; Chermprapai, A.; Patel, R. C. *J. Chem. Soc., Perkin Trans. 1* **1980**, 2901.
- Katritzky, A. R.; Zakaria, Z.; Lunt, E. J. *Chem. Soc., Perkin Trans. 1* **1980**, 1879.
- Benniston, A. C.; Rewinska, D. B. *Org. Biomol. Chem.* **2006**, *4*, 3886.
- Dilthey, W.; Quint, F.; Heinen, J. *J. Prakt. Chem.* **1939**, *152*, 49.
- Dilthey, W.; Quint, F.; Stephan, H. *J. Prakt. Chem.* **1939**, *152*, 99.
- Wu, D. Q.; Zhi, L. J.; Bodwell, G. J.; Cui, G. L.; Tsao, N.; Müllen, K. *Angew. Chem., Int. Ed.* **2007**, *46*, 5417.
- Claisen, L. *Ber. Dtsch. Chem. Ges.* **1887**, *20*, 665.
- Taljaard, B.; Goosen, A.; McClelland, C. W. S. *Afr. J. Chem.-S-Afr. T* **1987**, *40*, 139.
- Awad, S. B.; Abdulmalik, N. F.; Abdou, S. E. *Bull. Chem. Soc. Jpn.* **1975**, *48*, 2200.
- Abdulmalik, N. F.; Awad, S. B.; Sakla, A. B. *Bull. Chem. Soc. Jpn.* **1979**, *52*, 3431.
- Abdulmalik, N. F.; Awad, S. B.; Sakla, A. B. *Helv. Chim. Acta* **1979**, *62*, 1872.
- Hori, M.; Kataoka, T.; Asahi, Y.; Mizuta, E. *Chem. Pharm. Bull.* **1973**, *21*, 1415.
- Hori, M.; Kataoka, T.; Shimizu, H.; Hsu, C. F.; Hasegawa, Y.; Eyama, N. *J. Chem. Soc., Perkin Trans. 1* **1988**, 2271.
- Gilchrist, T. L. *Heterocyclic Chemistry*, 3rd ed.; Prentice Hall: New Jersey, NJ, 1997.
- Kastler, M.; Schmidt, J.; Pisula, W.; Sebastiani, D.; Müllen, K. *J. Am. Chem. Soc.* **2006**, *128*, 9526.
- Yang, X. Y.; Dou, X.; Rouhanipour, A.; Zhi, L. J.; Rader, H. J.; Müllen, K. *J. Am. Chem. Soc.* **2008**, *130*, 4216.
- Tanford, C. *J. Phys. Chem.* **1972**, *76*, 3020.
- Israelachvili, J. N.; Mitchell, D. J.; Ninham, B. W. *J. Chem. Soc., Faraday Trans.* **1976**, *72*, 1525.
- Israelachvili, J. N.; Mitchell, D. J.; Ninham, B. W. *Biochim. Biophys. Acta Bio-membr.* **1977**, *470*, 185.
- Kunitake, T.; Okahata, Y. *J. Am. Chem. Soc.* **1977**, *99*, 3860.
- Shimizu, T.; Masuda, M.; Minamikawa, H. *Chem. Rev.* **2005**, *105*, 1401.
- Perahia, D.; Traiphol, R.; Bunz, U. H. F. *Macromolecules* **2001**, *34*, 151.
- Oda, R.; Huc, I.; Schmutz, M.; Candau, S. J.; MacKintosh, F. C. *Nature* **1999**, *399*, 566.
- Faul, C. F. J.; Antonietti, M. *Adv. Mater.* **2003**, *15*, 673.
- Kato, T.; Mizoshita, N.; Kishimoto, K. *Angew. Chem., Int. Ed.* **2006**, *45*, 38.
- Binnemans, K. *Chem. Rev.* **2005**, *105*, 4148.